

Predicting RO/NF water quality by modified solution diffusion model and artificial neural networks

Yu Zhao^a, James S. Taylor^{b,*}, Shankar Chellam^c

^a URS Corporation, 7650 West Courtney Campbell Causeway Suite 700, Tampa, FL 33607-1462, USA

^b Department of Civil and Environmental Engineering, University of Central Florida, P.O. Box 162450, Orlando, FL 32816-2450, USA

^c Department of Civil and Environmental Engineering, University of Houston, Houston, TX 77204-4003, USA

Received 15 April 2004; received in revised form 20 March 2005; accepted 1 April 2005

Available online 23 May 2005

Abstract

Membrane solute mass transfer is affected by physical–chemical properties of membrane films, solvent (water) and solutes. Existing mechanistic or empirical models that predict finished water quality from a diffusion controlled membrane can be significantly improved. Modelling membrane solute mass transfer by diffusion solution model is generally restricted to developing specific solute mass transfer coefficients that are site and stage specific. A modified solution diffusion model and two artificial neural network models have been developed for modelling diffusion controlled membrane mass transfer using stage specific solute MTCs. These models compensate for the effects of system flux, recovery and feed water quality on solute MTC and predict more accurately than existing models.

© 2005 Elsevier B.V. All rights reserved.

Keywords: Diffusion; Water treatment; Neural network; Reverses osmosis

1. Introduction

Utilization of reverse osmosis (RO) and nanofiltration (NF) is increasing exponentially in drinking water treatment. Modelling of RO and NF performance is beneficial to pre-design studies, design and operation of membrane plants. The diffusion solution models are widely used to predict RO and NF performance. Solute mass transfer coefficients (MTC or K_s) are typically assumed to be constant in solution diffusion models, but are known to vary with influent water quality, operating conditions and intrinsic physical–chemical membrane properties which also vary with operation, quality and time. Solute specific $K_{s,s}$ vary by site and stage and limit modelling of membrane mass transfer.

Recent model developments include a non-linear description of the pressure differential and concentration differential across and through the membrane as well as the mathematical

integration of recovery into linear and film theory models [1–4]. However, since the effects of solute–solvent, solute–solute and solute–film interactions on solute mass transfer are essentially unknown, no mechanistic models have been developed that can compensate for these interactions. A previous investigation on pesticide removal by reverse osmosis found that the solute mass transfer coefficients could relate to system operation using flux and recovery. Hence, the solution diffusion model was modified by incorporating flux and recovery into solute mass transfer coefficient. The modified model predicted solute mass transfer (permeate concentrations) more accurately than the Solution Diffusion Model (SDM) for flat sheet, bench and pilot scale tests [5,6]. K_s is constant in the SDM and can be assumed constant in any model development; however, modification of K_s for varying flux and recovery produced a model that more accurately predicted permeate concentration in these instances. The flux, normalized MTC for water (K_w) and K_s are almost always larger for stage 1 than for stage 2. Typically the stage 1 driving force exceeds the stage 2 driving force because of energy losses associated with osmotic pressure and hydraulics.

* Corresponding author. Tel.: +1 407 823 2785; fax: +1 407 823 3315.
E-mail address: taylor@mail.ucf.edu (J.S. Taylor).

Recovery can also be related to energy losses associated with osmotic pressure and hydraulics.

Artificial neural network (ANN) models have been used to improve modelling mass transfer in RO or NF membrane processes. Most of ANN applications have modelled fouling [7–11]. Fewer ANN models have been developed for modelling membrane water quality. Historically the mass transfer of water has been described much more accurately than solute mass transfer in RO and NF processes. Niemi et al. [12] reported prediction of solute water quality using an ANN model was nearly the same as that obtained by using a diffusion controlled model for the separation of aqueous ethanol and acetic acid in a laboratory investigation. Bowen et al. [13] established an ANN model that accurately predicted salt rejection from salt solutions using nanofiltration in laboratory tests. Recently, Shetty and Chellam [10,11] reported development of a more universal membrane-specific ANN model using data from the information collection rule (ICR) database for different source waters and operating conditions using data from laboratory, pilot scale and full scale processes. This work significantly expanded the use of neural networks from laboratory treatment of a controlled solution to practical applications. Disadvantages of ANN models are the lack of information the model provides on mechanisms of mass transfer, the need for extensive data (limits the feasibility for general application), and all present ANN applications only use the multi-layer perceptron (MLP) model.

This paper compares actual and predicted permeate stream TDS using a conventional, modified conventional and two ANN models. The conventional and modified conventional models are the solution diffusion models and a modified solution diffusion based model (hybrid model) that modifies K_s using flux, recovery and net driving force (NDF). One ANN model uses MPL perceptron and the other ANN model uses a normal radial basis function for model development.

2. Theory

2.1. Solution diffusion model

The first model developed for a high recovery system was the linear homogenous solution diffusion model (HSDM), which was developed with six fundamental equations (Eqs. (1)–(5)) that considered a mass balance around the membrane element, pressure driven solvent and concentration gradient driven solute mass and recovery [1–5,14]. The HSDM is shown in Eq. (6). All solute mass transfer coefficients (K_s 's) in these models are overall K_s 's, which incorporate solute diffusivity and membrane thickness

$$F_w = K_w (\Delta P - \Delta \Pi) = \frac{Q_p}{A} \quad (1)$$

$$J_i = K_s \Delta C = \frac{Q_p C_p}{A} \quad (2)$$

$$R = \frac{Q_p}{Q_f} \quad (3)$$

$$Q_f = Q_c + Q_p \quad (4)$$

$$Q_f C_f = Q_c C_c + Q_p C_p \quad (5)$$

$$C_p = \frac{C_f K_s}{K_w (\Delta P - \Delta \pi) \left(\frac{2-2R}{2-R} \right) + K_s} \quad (6)$$

Specific developments of mass transfer models have included non-linear modification of pressure and concentration differentials across and through the membrane as well as integration of recovery and incorporation of film theory into models predicting permeate concentration [1–5,14,15].

The film theory model describes mass transfer through the membrane using films on the feed and permeate sides of the membrane, which results in increased solute concentration relative to the bulk on the feed side and is known as concentration polarization. The steady state HSDM as modified by film theory (HSDM-FT) is shown in Eq. (7):

$$C_p = \frac{C_f K_s e^{F_w/k_b}}{K_w (\Delta P - \Delta \pi) \left(\frac{2-2R}{2-R} \right) + K_s e^{F_w/k_b}} \quad (7)$$

The solute mass transfer coefficient is assumed constant in both the HSDM (Eq. (6)) and the HSDM-FT (Eq. (7)). However, in tradition linear and film theory models, all solute mass transfer coefficient are assumed constant and do not change during integration.

The linear approximation of the non-linear concentration profile of the membrane feed stream incorporated a known error into the HSDM and HSDM-FT. Mulford et al. [3] developed an integrated HSDM (IHSDM) by developing, integrating and incorporating a differential equation relating instantaneous feed stream concentration into the HSDM and HSDM-FT. The IHSDM and IHSDM-FM are as presented in Eqs. (8) and (9):

$$C_p = \frac{K_s C_f}{-R F_w} \ln \left(1 - \frac{R F_w}{F_w + K_s} \right) \quad (8)$$

$$C_p = \frac{K_s C_f}{-R F_w e^{F_w/k_b}} \ln \left(1 - \frac{R F_w}{F_w + K_s e^{F_w/k_b}} \right) \quad (9)$$

The HSDM and IHSDM do not compensate for any variations in pressure, osmotic pressure or flux through the membrane elements or arrays. The recently developed incremental diffusion model (IDM), and integrated osmotic pressure model (IMOP) model [16] do consider changes in flux, pressure and osmotic pressure through the membrane elements and arrays. Those models without and with incorporation of film theory are shown in Eqs. (6)–(9). The IDM and IMOP are shown in Eqs. (10) and (11). The IDM-FT and IMOP-FT are shown in Eqs. (12) and (13):

$$C_p = \frac{C_{f_0}}{R} [1 - (1 - R)^{K_s/(F_w + K_s)}] \quad (10)$$

$$C_p = \frac{C_f}{R} \left\{ 1 - \left[\left(\frac{\Delta P - \Delta \Pi_{out}}{\Delta P - \Delta \Pi_{in}} \right) (1 - R) \right]^{K_s / (K_w \Delta P + K_s)} \right\} \quad (11)$$

$$C_p = \frac{C_{f0}}{R} [1 - (1 - R)^{(F_w(1 - e^{F_w/k_b}) + K_s) / (F_w + K_s)}] \quad (12)$$

$$C_p = \frac{C_f}{R} \left\{ 1 - \left(\frac{\Delta P - \Delta \Pi_{out}}{\Delta P - \Delta \Pi_{in}} \right)^{K_s / (K_s + K_w \Delta P)} \right. \\ \left. \times (1 - R)^{1 - (e^{F_w/k_b} K_w \Delta P) / (K_s + K_w \Delta P)} \right\} \quad (13)$$

2.2. Modified solution diffusion model

NF and RO membranes were shown to remove pesticides in a field study supported by Taylor et al. [6]. Pesticide concentration in the permeate stream was diffusion controlled but the error for pesticide prediction using the HDSM model was systematically related to flux and recovery. Prediction of pesticides in the permeate stream were improved by modifying K_s which is a hybrid model where K_s was modified by incorporation of flux and recovery. This hybrid model is a solution diffusion based model that incorporated factors that impacted K_s . There are numerous model equations can be developed in this manner.

A good hybrid model must meet specific requirements even though it may be partly or totally empirical. A good hybrid model should be sensitive to factors that change K_s such as flux and recovery. A good hybrid model should have physical meaning for ranges of independent variables that are not uncommon to normal operation, but may be beyond the range of the original data. Mathematically correct models will converge at all mathematically feasible operational environments. The close-to-linear and non-linear model was used to ensure model convergence for screening model equations [17]. The new hybrid model equations are based on solution diffusion model and compensate for flux, recovery and net driving force parameters that are common to membrane plant operation.

A hybrid model for K_s is shown in Eq. (14). The K_s model was developed from the IDM by trial and error, and emphasizes the effect of flux more than recovery on K_s . This model is diffusion based and has only one unknown model coefficient and one unknown model exponent. Eq. (14) can be substituted in any model that utilizes a solute mass transfer coefficient to predict permeate stream solute concentration in a diffusion controlled membrane process. To avoid unreasonable model predictions, model validation also was checked at extended boundaries, such as $K_s > 0$ at 0 and 90% recovery and flux > 0 .

$$K_s = \frac{F_w^A \ln(1 - BR)}{\ln(1 - R) - \ln(1 - BR)} \quad (14)$$

where $A > 0$, $B < 1$.

2.3. ANN models

Neural networks can predict any continuous relationship between inputs and the target. Similar to linear or non-linear regression, artificial neural networks develop a gain term that allows prediction of target variables for a given set of input variables. Physical–chemical relationships between input variables and target variables may or may not be built into the association of target and input variables.

Two types of ANN models for K_s are described in this work. The models use the same input parameters as the theoretical solution diffusion models and the hybrid model. K_s s developed by regression and ANN can be compared, or can be inserted in existing solute mass transfer models and accuracy of the predicted permeate solute concentrations can be easily compared.

2.3.1. Multilayer perceptron model

Multilayer perceptron (MLP) is the most common type of neural network used for supervised prediction. Most of the previous literature describing membrane models used MLPs. A MLP is a feed-forward neural network that uses a sigmoid activation function, i.e. the hyperbolic tangent. The following is a simple MLP model with one hidden layer containing two hidden neurons. The general form of a feed-forward neural network expresses a transformation of the expected target (here C_p) as a linear combination of non-linear functions of linear combinations of the inputs (here feed water quality C_f , system flux (F_w) and recovery (R)).

$$g_0^{-1}(E(C_p)) = w_0 + w_1 H_1 + w_2 H_2$$

$$H_1 = \tanh(w_{01} + w_{11} C_f + w_{21} F_w + w_{31} R)$$

$$H_2 = \tanh(w_{02} + w_{12} C_f + w_{22} F_w + w_{32} R)$$

$$\tanh(x) = \frac{e^x - e^{-x}}{e^x + e^{-x}}$$

where $g_0^{-1}(E(C_p))$ is the transformation of the expected target as the inverse of output activation function, and equals combination functions (here linear combinations) for the arguments of activation functions. The w_1 , w_{11} , w_{12} represents weights and w_0 , w_{01} , w_{02} are bias which are estimated by fitting model to data.

2.3.2. NRBF model

A normalized radial basis function (NRBF) network is a feed-forward network with a single hidden layer using the softmax activation function, which is applied to a radial combination of inputs. In contrast to MLP, each basis function is the ratio of a bell-shaped Gaussian surface to sum of Gaussian surfaces. The following is a NRBF model containing two hidden neurons. The transformation of the expected target (C_p) is a linear combination of softmax functions of non-linear

combinations of the inputs (C_f , F_w and R).

$$g_0^{-1}(E(C_p)) = w_1 H_1 + w_2 H_2$$

$$H_1 = \frac{e_1}{e_1 + e_2}, \quad H_2 = \frac{e_2}{e_1 + e_2}$$

$$e_i = \exp(f \ln(a_i) + w_{0i}((C_f - w_{1i})^2 + (F_w - w_{2i})^2 + (R - w_{3i})^2))$$

For the model NRBF given equal width and height (NRBFEQ), $a_i = 1$, the combination function becomes:

$$e_i = \exp(w_{0i}^2((C_f - w_{1i})^2 + (F_w - w_{2i})^2 + (R - w_{3i})^2))$$

where w_{0i} , w_{1i} and w_{2i} represents weights which are estimated by fitting model to data.

3. Data

Data from USEPA information collection rule (ICR) database [18,19] was used for this study that was collected from a nine MGD two-stage nanofiltration plant located in Palm Beach County in Florida. Using data from a full-scale membrane plant for model development and verification benefits future model utilization by the water community. The general information for this full-scale membrane plant is summarized in Table 1.

Experimental data from 12 March 1998 to 16 March 1999 provided more than 8800 h observations of run time and 706 observations for stage 1 (354 observations) and stage 2 (352 observations) TDS. A summary of statistical operating data for flux, recovery, net driving force, feed and permeate stream TDS is shown in Table 2. The range and variation of flux, recovery and NDF as shown in Table 2 are typical of a nanofiltration plant operating at steady state on a groundwater source.

Table 2
Summary of water quality and operating condition

	Feed TDS (mg/L)	Permeate TDS (mg/L)	Flux (gsfd)	Recovery	NDF (psi)
					<i>Stage1</i>
Mean	341.5	50.4	13.6	55.2%	81.3
S.D.	15.2	6.9	0.4	0.1%	1.3
Min.	301.3	42.0	12.5	54.0%	72.4
Max.	587.0	71.0	14.9	56.5%	84.8
					<i>Stage2</i>
Mean	720.2	115.0	13.2	66.5%	46.1
S.D.	9.7	7.1	0.4	0.3%	1.2
Min.	690.0	104.0	12.1	65.2%	42.7
Max.	747.0	164.0	14.4	69.9%	49.0

1 kPa = 0.145 psi; 1 L m⁻² h⁻¹ = 0.589 gsfd.

Table 1
General information of verification data source

Membrane plant	Palm Beach County
Scale	Full-scale
Array	Two-stage array
Source	Ground water
Run time (h)	0–8856
Capacity	9.32 MGD (35,000 m ³ /day)
Manufacturer	Koch
MWC ^a	200
Material	Polyamide
Construction	TFC ^b

^a Molecular weight cut-off (Da).

^b Thin film composite.

4. Model procedure

The following procedure was used for model development:

- Seventy percent of the stages 1 and 2 data were randomly selected for model development. The remaining 30% of the data were used for model verification. K_s values and other unknown parameters for the HSDM, IHSDM, IDM, IMOP and film theory models were determined by non-linear regression of the development data set using Eq. (6)–(13).
- Outliers for target variables K_s and flux, recovery and NDF detected and discarded by the cook distance or Cove ratio procedures.
- The model fitting statistics included t -statistics for significant model parameters coefficients, t -tests of paired samples demonstrate the significance between model predicted and actual values and Pearson numbers for model fit of actual and predicted data.
- Validation statistics: similar to the model fitting statistics but uses data that were not used for model development.
- Model extrapolation: check model predictions in the expanded range of recovery and flux.
- Neural network models are evaluated in the same manner as regression models. The same data and parameter testing is used for experimental and expanded data ranges.

- The neural network model developed in this paper was based on software SAS Enterprise Miner.

5. Results and discussion

5.1. Solution diffusion model

All mass transfer coefficients in all models (K_w , K_s and k_b) were determined using non-linear regression. The values for these models represent the statistical fit for each that produces the least error for prediction using the regression data set. As previously noted, k_b is present in the numerator and denominator of the film theory models, which limits the impact of k_b . K_w , K_s and k_b mass transfer coefficients were verified using independent data to predict solute concentration. The mass transfer coefficients that were developed by non-linear regression for the HSDM, IHSDM, IDM and IMOP with and without film theory are shown in Table 3. The data set containing 70% of the total data was used for non-linear regression and model development, the remaining 30% of the data was used for verification.

The large k_b values in Table 3 mean the concentration polarization effect represented by k_b in the film theory models is not significant. The large exponents reduce the film theory concentration factor to one and the film theory models become identical to the solution diffusion models that did not incorporate film theory. The k_b 's determined using from large and small scale investigations differed significantly. One reason for this is the lack of impact that k_b has on the prediction of C_p , because k_b appears in the numerator and denomina-

Table 3

Solution diffusion model results

Model	K_s (gsfd)	k_b (gsfd)
HSDM	1.249	
IHSDM	1.520	
IDM	1.483	
IMOP	1.548	
HSDM-FT	1.249	9.99×10^{10}
IHSDM-FT	1.520	6.87×10^7
IDM-FT	1.483	1.76×10^{10}
IMOP-FT	1.548	1.15×10^9

$1 \text{ L m}^{-2} \text{ h}^{-1} = 0.589 \text{ gsfd}$.

tor of the film theory models, which is quickly determined by statistical regression programs and shown in these results. Another reason for the difference, is the expected differences from laboratory and field investigation due to difference in hydraulics, configuration and other performance related parameters that differ in the field and laboratory. k_b can be determined from the Sherwood number ($Sh = a Re^b Sc^{1/3}$) given a , b and c are determined by regression or from the literature, but have been shown to inaccurately predict field performance of membrane processes [4–6].

The actual versus predicted permeate stream TDS is shown in Fig. 1 by stage for the HSDM, IHSDM, IDM and IMOP models using the independent verification dataset. The 45° line in Fig. 1 is the line that represents a plot of actual versus predicted TDS if there were no error. The predicted versus actual TDS is clustered into stages 1 and 2 groups. Although R^2 based on a combined stages 1 and 2 data set was greater than 0.9, R values based on individual stage data were negative

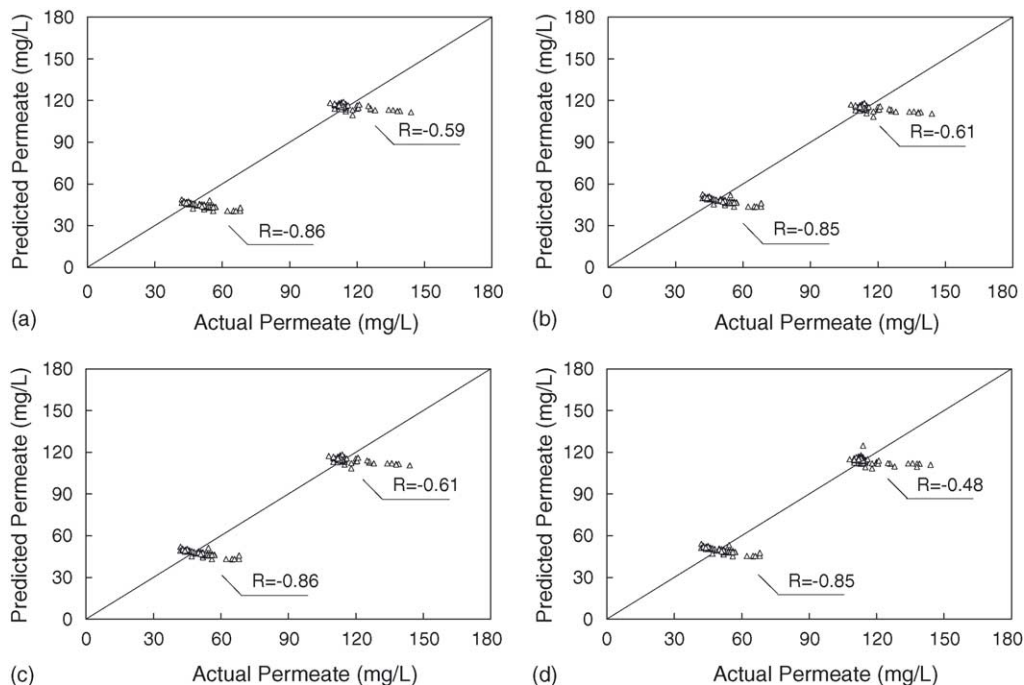


Fig. 1. Model predicted vs. actual permeate TDS concentration (mg/L) for the HSDM (a), IHSDM (b), IDM (c) and IMOP (d) models.

Table 4
Hybrid model results

Parameter	Estimate	S.E.	Lower (95% CI)	Upper (95% CI)
A	2.59	0.149	2.30	2.88
B	0.0026	0.00099	0.00061	0.0045

and are shown in Fig. 1. No significant difference was found for the predicted and actual TDS for any of these models using a paired *t*-test. The high R^2 indicates these models can be used effectively for prediction, but a negative *R* for each stage indicates the models could be improved. The models over predicted the actual TDS for low TDS observations and under predicted actual TDS for high TDS observations, which is a common fault of predictive models for solute mass transfer in RO or NF membranes. Certainly, these models can be used but clearly they can be improved.

5.2. Hybrid and ANN model development

Estimates of the unknown parameters for the hybrid model shown in Eq. (14) were determined using non-linear regression and are presented in Table 4. Model verification was determined by conducting a paired *t*-test on the predicted and actual TDS using the independent data set. As shown by the paired *t*-tests and Fig. 2, there was no difference between predicted and actual TDS for the hybrid or ANN models. The correlation coefficient for each stage data set is positive and indicates significant model predictability. R^2 for the combined stages 1 and 2 data set was 0.98.

A comparative study between the ANN models which set target variable C_p directly (C_p model) against the ANN

Table 5
Summarized K_s statistics for ANN C_p model and ANN K_s model

	Overall R^2	Stage 1 <i>R</i>	Stage 2 <i>R</i>
MLP- C_p	0.99	0.83	0.77
NRBSEQ- C_p	0.99	0.8	0.85
MLP- K_s	0.99	0.77	0.78
NRBSEQ- K_s	0.99	0.76	0.79

Where MLP- C_p represents direct C_p MLP model, and MLP- K_s represents direct K_s ANN model and so on.

models using K_s as target variable (K_s model) in conjunction with HSDM model was done. The predicted versus actual permeate concentration by these two procedures showed the ANN C_p model is superior to the ANN K_s model. Table 5 summarizes the correlations for stages 1 and 2 and R^2 value for combined stages between model predicted and actual C_p . Clearly, although R^2 are all very high (0.99), the direct C_p model had better *R* values than the K_s model. The ANN MLP and NRBSEQ model results are shown in Table 6. Development of the ANN models was done by processing paired TDS permeate stream concentrations, flux, recovery and TDS feed stream concentrations using SAS Enterprise Miner to develop the results shown in Table 5 for development of the MLP and NRBSEQ models. The ANN MLP and NRBSEQ models describe C_p as a function of flux, recovery and feed stream TDS. These models could be utilized manually by calculating H_1 and H_2 , then using H_1 and H_2 to determine the C_p inverse activation function, which allows direct calculation of C_p . However, practical application of these models would be best achieved by simply inputting the values shown in Table 5 in one of the several computer programs, which

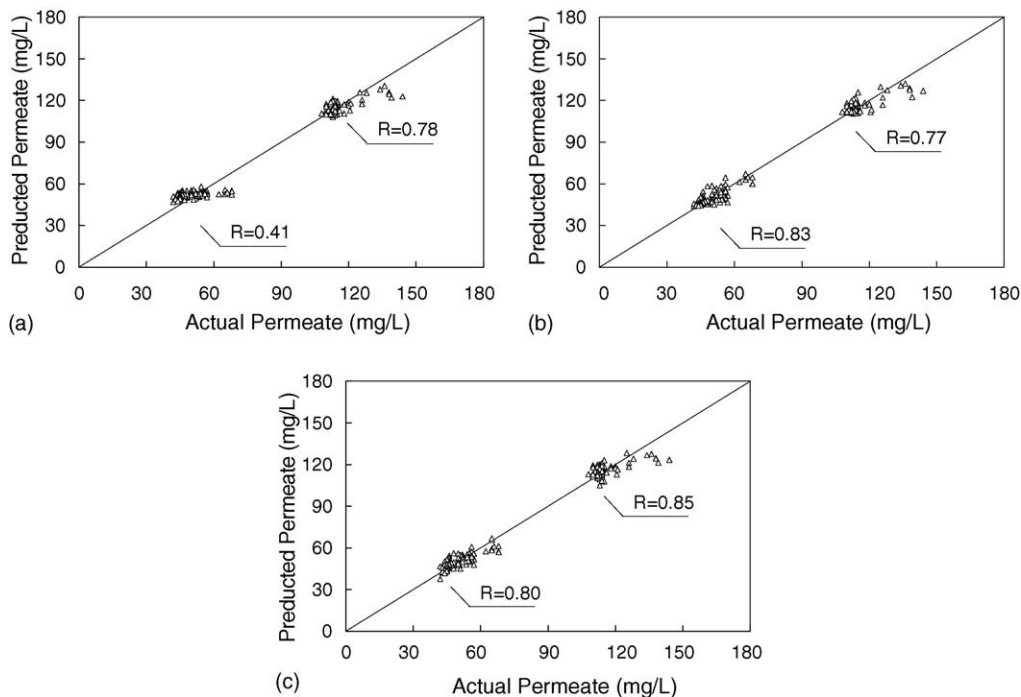


Fig. 2. Actual vs. predicted TDS using data not used for model development for the HHSDM (a), MLP (b) and NRBSEQ (c) models.

Table 6
MLP and NRBFEQ model results

MLP weighted variables			NRBSEQ weighted variables		
Name	Var1	Weight	Name	Var1	Weight
$C_f \cdot H_{11}$	w_{11}	1.0997	$C_f \cdot H_{11}$	w_{11}	-0.11333
Flux_ H_{11}	w_{21}	-0.9117	Flux_ H_{11}	w_{21}	-0.0767
Recovery	w_{31}	-1.3595	Recovery	w_{31}	-0.25441
$C_f \cdot H_{12}$	w_{12}	22.804	$C_f \cdot H_{12}$	w_{12}	-0.14478
Flux_ H_{12}	w_{22}	1.8891	Flux_ H_{12}	w_{22}	0.025737
Recovery	w_{32}	9.7523	Recovery	w_{32}	0.27545
Bias_ H_{11}	w_{01}	0.8581	Bias_ H_{11}	w_{01}, w_{02}	1.1203
Bias_ H_{12}	w_{02}	-1.3692	$H_{11} \cdot C_p$	w_1	20.534
$H_{11} \cdot C_p$	w_1	-12.153	$H_{12} \cdot C_p$	w_2	146.76
$H_{12} \cdot C_p$	w_2	33.009			
Bias_ C_p	w_0	89.155			

are capable of processing ANN models such as SAS or Matlab.

Actual and predicted TDS from the hybrid, MLP and NRBSEQ model verification is shown in Fig. 2. Immediately obvious is the improved grouping for the actual and predicted TDS using the hybrid, MLQ and NORFEQ models. All correlation coefficients were positive. The NORFEQ model had the highest R^2 . Again, paired sample t -tests showed no significant differences between the predicted and actual permeate concentrations using any of the models, and hence all models were verified using the independent data set.

Prediction of C_p versus flux and recovery is shown in Fig. 3 assuming 1000 mg/L TDS in the feed stream for the hybrid, MLP and NRBFEQ models. The C_p predicted plane using the hybrid model is very smooth and has no striking C_p change for varying flux and recovery. However, the hybrid model provided the least accurate prediction of C_p . The MLP and

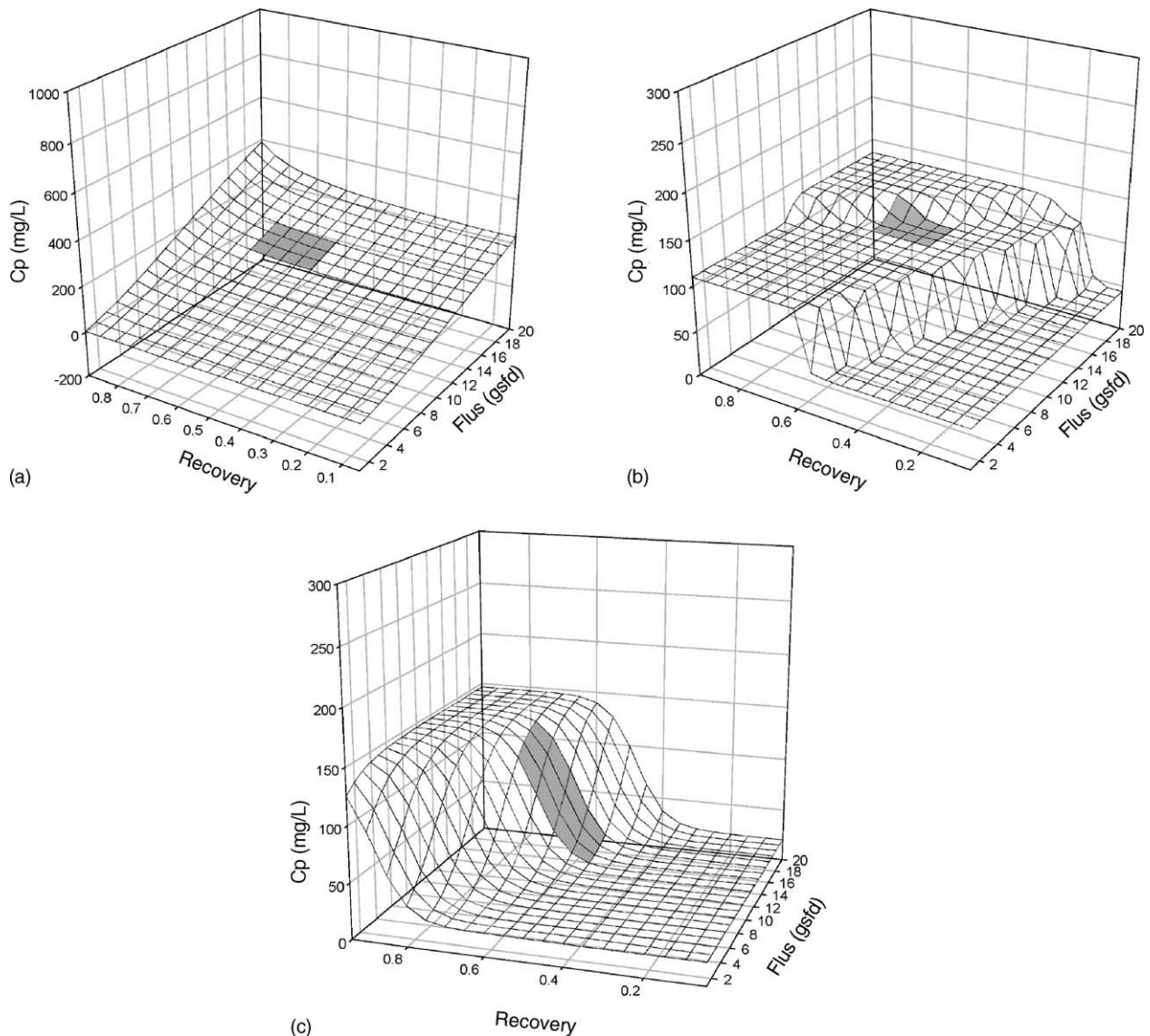


Fig. 3. Permeate TDS predicted by hybrid (a), MLP (b) and NRBFEQ (c) models. The shaded area represents the variation scope of original data.

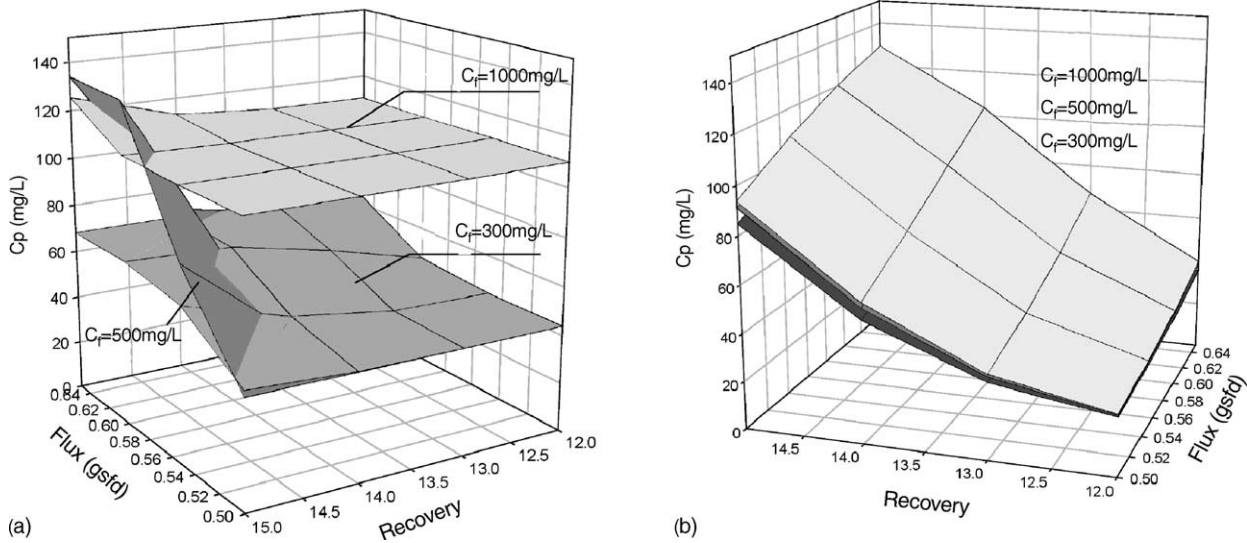


Fig. 4. Permeate TDS predicted MLP (a) and NRBFEQ (b) models at feed TDS 300, 500 and 1000 mg/L.

NRBFEQ are neural network models and produced predicted C_p s that changed dramatically at selected fluxes and recoveries. The MLP model predictions for C_p almost appear like a step function at 60% recovery and 2 gsf/d going from 50 to 100 mg/L. This trend can be clearly seen in Fig. 3(b). Another similar change is seen in the back section of the predicted C_p plane in Fig. 3(b). The NRBFEQ model predicted a C_p dramatically but smoother changing C_p than the MLP model. NRBFEQ predicted C_p s increased from 50 mg/L at 80% recovery to 130 mg/L at 90% recovery. It is likely that the ANN models would change if actual data from the extended independent variable ranges were used in model development.

Prediction of C_p at various feed TDS concentration is shown in Fig. 4 for the MLP and NRBFEQ models. The three layers from top to bottom in Fig. 4(a) and (b) represent prediction at feed TDS 300, 500 and 1000 mg/L. Clearly, when feed concentration is within the intermediate range of actual feed concentration (300–800 mg/L, e.g. 500 mg/L), MLP and NRBFEQ model predict in similar manner; however, the prediction diverge at 300 and 1000 mg/L feed concentration, MLP is a model weighed more on C_f , while NRBFEQ is more weighted on operating conditions.

6. Conclusions

- Several diffusion based, hybrid and two ANN models were developed for predicting permeate TDS using an ICR database from a full-scale nanofiltration plant.
- All concentration polarization or film theory terms were insignificant.
- All diffusion based models that did not consider concentration polarization, hybrid and ANN models were verified by comparing actual and predicted data using a t -test.
- The diffusion based models over predicted TDS at low TDS concentrations and under predicted TDS at high TDS

- concentrations, which is typical of diffusion based models.
- The hybrid and ANN models predicted permeate TDS more accurately than any of the diffusion based models, and did not over or under predict permeate TDS at low and high permeate TDS.
- Although ANN models are not mechanistically based, these models did predict dramatic changes in permeate TDS for certain combinations of flux and recovery. Such phenomena can be investigated at extended ranges of flux and recovery and could give new insight into mechanisms affecting membrane mass transfer.
- Numerous hybrid and ANN models can be developed and could significantly improve prediction of membrane performance.

Nomenclature

C_c	concentrate concentration (M/L ³)
ΔC	concentration gradient (M/L ³)
C_f	feed concentration (M/L ³)
C_{f_0}	feed stream solute concentration at membrane inlet (M/L ³)
ΔC_f	feed solute concentration (M/L ³)
C_p	permeate concentration (M/L ³)
F_w	water flux through the membrane (L/t)
J_i	solute flux (M/L ² t)
k_b	back diffusion mass transfer coefficient from the surface to the bulk
K_s	solute mass transfer coefficient (L/t)
K_w	solvent mass transfer coefficient (L ² t/M)
P_{in}	static pressure at inlet (L)
P_{out}	static pressure at outlet (L)
P_p	static pressure in permeate stream (L)
ΔP	pressure gradient (L)

Q_c	concentrate stream flow (L^3/t)
Q_f	feed stream flow (L^3/t)
Q_p	permeate stream flow (L^3/t)
r	recycle rate (fraction)
R	recovery (fraction)

Greek letters

Π	osmotic pressure (L)
$\Delta\Pi$	osmotic pressure difference (L)
$\Delta\Pi_{in}$	bulk osmotic pressure difference at membrane inlet (L)
$\Delta\Pi_{out}$	bulk osmotic pressure difference at membrane outlet (L)

References

- [1] J.S. Taylor, Membrane, in: Water Quality and Treatment, AWWA, Denver, CO, 1999 (Chapter 11).
- [2] J.S. Taylor, M. Jacobs, Water treatment membrane processes, in: J. Malevalle, P. Odendaal, M. Wiesner (Eds.), Reverse Osmosis and Nanofiltration, McGraw-Hill, New York, 1996 (Chapter 9).
- [3] L.A. Mulford, J.S. Taylor, D. Nickerson, S.S. Chen, Comparison of full- and pilot-scale nanofiltration on plant performance, J. AWWA 91 (6) (1999) 64–75.
- [4] S. Chellam, J.S. Taylor, Simplified analysis of contaminant rejection during ground and surface water nanofiltration under the information collection rule, Water Res. 35 (10) (2001) 2460–2474.
- [5] S.S. Chen, Modelling of membrane surface chemistry and mass transfer, Ph.D. Dissertation, University of Central Florida, 1999.
- [6] J.S. Taylor, X.S. Chen, L.A. Mulford, C.D. Norris, Flat Sheet, Bench and Plot Testing for Pesticide Removal Using Reverse Osmosis, AWWA Research Foundation, 1998.
- [7] N. Delgrange, C. Cabassud, M. Cabassud, L. Durand-Bourlier, J.M. Laine, Modelling of ultrafiltration fouling by neural network, Desalination 118 (1998) 213–227.
- [8] C. Teodosiu, O. Pastravanu, M. Macoveanu, Neural network models for ultrafiltration and backwashing, Water Res. 34 (18) (2000) 4371–4380.
- [9] M. Cabassud, N. Delgrange-Vincent, C. Cabassud, L. Durand-Bourlier, J.M. Laine, Neural networks: a tool to improve UF plant productivity, Desalination 145 (2002) 223–231.
- [10] G.R. Shetty, H. Malki, S. Chellam, Predicting contaminant removal during municipal drinking water nanofiltration using artificial neural networks, J. Membr. Sci. 212 (2003) 99–112.
- [11] G.R. Shetty, S. Chellam, Predicting fouling of nanofiltration membranes during municipal drinking water treatment using artificial neural networks, J. Membr. Sci. 217 (1–2) (2003) 69–86.
- [12] H. Niemi, A. Bulsari, S. Palosaari, Simulation of membrane separation and neural networks, J. Membr. Sci. 102 (1995) 185–191.
- [13] W.R. Bowen, M.G. Jones, J.S. Webfoot, H.N.S. Yousef, Predicting salt rejection at nanofiltration membranes using artificial neural networks, Desalination 129 (2000) 147–162.
- [14] J.S. Taylor, L.A. Mulford, S.J. Duranceau, W.M. Barrett, Cost and performance of a membrane pilot plant, J. AWWA 81 (11) (1989) 52–60.
- [15] L. Sung, Film theory and ion coupling models for a diffusion controlled membrane process, Ph.D. Dissertation, University of Central Florida, 1993.
- [16] Y. Zhao, Modelling of membrane solute mass transfer in NF/RO membrane systems, Ph.D. Dissertation, University of Central Florida, 2004.
- [17] D.A. Ratkowsky, Handbook of Nonlinear Regression Models, Marcel Dekker, 1990.
- [18] USEPA ICR Treatment Study Database, Office of Ground Water and Drinking Water, Cincinnati, OH, 2000.
- [19] USEPA, ICR Manual for Bench- and Pilot-scale Treatment Studies, Office of Ground Water and Drinking Water, Cincinnati, OH, 1996, 1-1-3-108.